INDIAN JOURNAL OF SCIENCE AND TECHNOLOGY

RESEARCH ARTICLE

Synthesis, Optical, Electrical, Fluorescence, Dielectric, Thermal, and Mechanical Characterization of 3-Aminopyridine (Scaffold in Drugs) Single Crystal

I Shubashini[1], **S Robinson Jebas**[2]*

1 Research Scholar (Reg No: 21111062132003), PG and Research Department of Physics, Kamarajar Government Arts College, (Affiliated to Manonmaniam Sundaranar University), Surandai, Tenkasi Dt, 627859, Tamil Nadu, India
2 Associate Professor, PG and Research Department of Physics, Kamarajar Government Arts College, Surandai, Tenkasi Dt, 627859, Tamil Nadu, India

OPEN ACCESS

Received: 29-08-2024
Accepted: 27-09-2024
Published: 18-10-2024

Citation: Shubashini I, Jebas SR (2024) Synthesis, Optical, Electrical, Fluorescence, Dielectric, Thermal, and Mechanical Characterization of 3-Aminopyridine (Scaffold in Drugs) Single Crystal . Indian Journal of Science and Technology 17(39): 4119-4128. https://doi.org/10.17485/IJST/v17i39.2789

* **Corresponding author**.

jebas2@gmail.com

Funding: None

Competing Interests: None

Published By Indian Society for Education and Environment (iSee)

ISSN
Print: 0974-6846
Electronic: 0974-5645

Abstract

Objectives: To screen the optical, electrical, fluorescence, dielectric, thermal, and mechanical behavior of the 3-aminopyridine single crystal for its suitability in optoelectronic applications. **Methods:** A good single crystal of 3-aminopyridine (3-AP) was grown by the slow evaporation method. **Findings:** The lattice parameters of the grown crystal were determined using a single crystal X-ray diffractometer as, a = 6.184 (4) Å, b = 15.350 (6) Å, c = 5.361 (7) Å and the required functional groups C-N, NH_2 bonds of 3-AP were recognized by the FTIR studies. The grown crystal was screened using the UV-Vis-NIR spectrum to understand the transmission and absorption character of the crystal. The various optical constants such as absorption coefficient, optical conductivity, and electrical conductivity of the crystal have been determined from the UV-Vis transmission plot. The lower cut-off wavelength of the 3-AP crystal was observed at 250 nm. The band gap of the grown crystal is found to be 4.5 eV. The emission property of the crystal was studied using fluorescence spectra. Violet, blue, and red emissions are observed from the fluorescence spectra. Thermal screening of the 3-AP crystal was performed using TGA and DTA. The 3-AP crystal remains stable up to 220 ºC and then the crystal begins to decompose up to 260 ºC due to the loss of the -NH_2 group of the 3-aminopyridine. The Vickers hardness test revealed the nature of the material as soft type with Meyer's index (n) of 2. The electronic polarization behavior of the crystal was examined using the dielectric study. **Novelty:** The lower cut-off wavelength of 250 nm, wide band gap of 4.5 eV, excellent transparency in the entire visible and near-infrared region, violet, blue, and red emission by the material are the distinguishing and mandatory features for optoelectronic applications. These features are good as compared to the 3-AP derivatives reported earlier.

Keywords: Unit cell; Absorption; Emission; Conductivity; Strength; Loss

1 Introduction

Crystals play an important role in the field of semiconductors and optoelectronics. The research in the development of novel organic materials is advancing tremendously owing to the many advantages of organic crystals the ease of processing in the assembly of optical devices, high NLO coefficient, large laser damage threshold, wide optical transparency, large hyperpolarizability, and high thermal stability[1]. Organic crystals with excellent optical properties are being used in the fields of optical communication, frequency doubling, photonics, and optoelectronics device fabrication[2]. One of the interesting features of organic crystals is that the chemical structure of the molecular compound can be tuned to get the desired emission wavelength[3].

Pyridine and their organic derivatives display a large amount of fluorescence in the crystalline state, being used in signal transmission processing and laser printing[4]. In the recent, optical characteristics of amino pyridine derivatives and their utility for the fabrication of optoelectronic devices were reported[5]. The optical properties of amino pyridine (AP) complexes and their use for the fabrication of optoelectronic devices have been reported[6]. Pyridine is a scaffold in various natural products, drug molecules, and vitamins. Pyridine scaffolds are found in nature, mainly from plant resources such as alkaloids and one of the most effective cholinergic drugs atropine (Atropa belladonna), which holds a saturated pyridine ring.[7]. The nonlinear optical behavior of the 3-aminopyridine derivatives such as 3-aminopyridinium 2-amino 5-chloro pyridine, 3, 5-dinitrobenzoate, 3-aminopyridine 4-nitrophenol, 3-aminopyridine 2, 4-dinitrophenol, and 3-aminopyridine picrate, 2-amino pyridinium phthalate, 2-aminopyridinium fumarate fumaric acid has been reported in the literature[8–14].

The applications of pyridine derivatives in optoelectronics, catalytic, photophysical, organic semiconductors, and electrochemical fields have been reported[15]. The crystal structure of 3-AP has already been reported in the literature[16] with the lattice parameters of a = 6.186 (4) Å, b = 15.298 (6) Å, c = 5.713 (7) Å, β = 110.54 (2)°. The literature indicates numerous uses for pyridine derivatives; however, the optical, electrical, dielectric, and mechanical properties of 3-aminopyridine have not been characterized.

To understand the optical, electrical, dielectric, and mechanical behaviour of 3-aminopyridine we have done the various characterization, and the results are presented here. The computation of various optical constants and wide transparency windows indicates that the 3-aminopyridine crystal is suitable for optoelectronic device fabrication.

2 Methodology

3-Aminopyridine (3g) (AR grade Merck) was dissolved in 30 ml water. The mouth of the beaker was closed with silver paper and minute holes were put to pave the slow evaporation of the transparent solution obtained. After five weeks brown color crystals were obtained. Figure 1 shows the photograph of 3-AP single crystal.

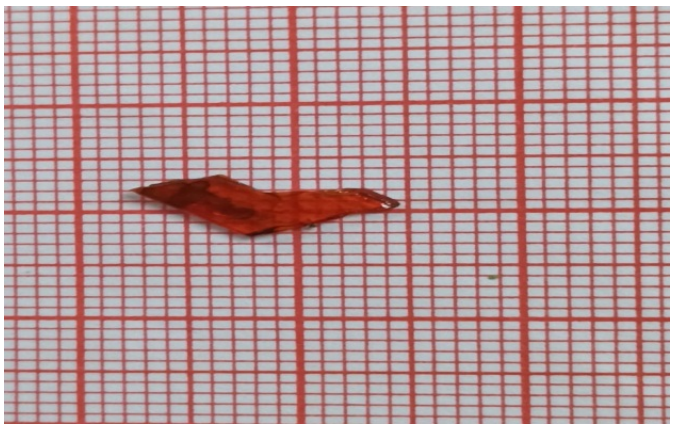

Fig 1. Photograph of 3-AP crystal

3 Result and Discussion

3.1 Single Crystal X-Ray Diffraction

Single crystal X-ray diffraction study was performed using BRUKER Q8 QUEST Duo X-ray diffractometer. The crystal system and space group were found to be monoclinic with $P2_1$. The lattice parameter of the 3-aminopyridine crystal was determined as, a = 6.184 (4) Å, b = 15.350 (6) Å, c = 5.361 (7) Å, α = 90.57 (11) °, β = 107.39 (20) °, and γ = 90.35 (10) °.

3.2 FTIR Analysis

The Fourier Transform Infrared spectrum of 3-AP single crystal was recorded in a Perkin-Elmer Spectrometer in the range of 4000 cm^{-1} to 400 cm^{-1} using the KBr pellet technique. The C-N stretching vibration is in the region of 1382-1266 cm^{-1} for aromatic amines[17]. Here the peak at 1361 cm^{-1} is assigned to aromatic C–N stretching. At 3349 cm^{-1}, the symmetric NH_2 stretching is detected. The range at 1585 cm^{-1} is where the NH_2 in-plane deformation vibration is noticed. At 3217 cm^{-1}, the symmetric NH stretching is detected[17]. Figure 2 shows the FTIR spectrum of 3-aminopyridine crystal.

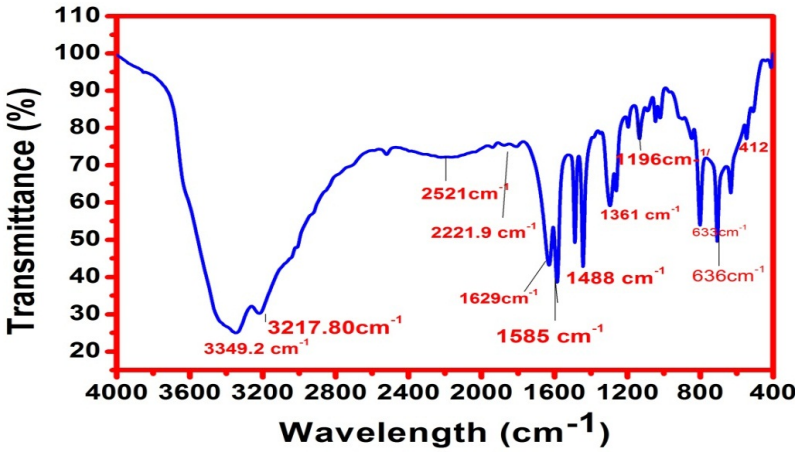

Fig 2. FTIR spectrum of 3-AP

3.3 UV-Visible NIR Analysis

The optical transmittance spectrum of a 3-AP single crystal was recorded using a Perkin Elmer Lambda 35 spectrophotometer in the wavelength range of 200 nm to 1100 nm. The optical transmittance spectrum is shown in Figure 3. The lower cut-off wavelength of the 3-AP crystal was observed at 250 nm. The spectrum shows 90% transparency in the entire visible and near-infrared region and there is no significant absorption, suggesting the purity and suitability of the 3-AP crystal for optoelectronic device fabrication.

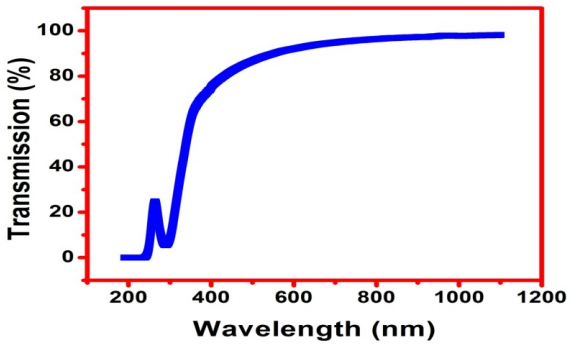

Fig 3. Optical transmission spectrum of 3-AP

3.3.1 Optical Band Gap Energy (Eg)

The atomic and electronic band structures of the produced crystals are proportional to the optical band gap energy[18]. Using equation[19], the optical absorption coefficient (α) was determined.

$$\alpha = \left(\frac{2.3036}{t}\right) log\frac{1}{T} m^{-1} \tag{1}$$

Where t is the crystal's thickness and T is its transmittance. The optical band gap energy (E_g) is related to the absorption coefficient (α) and photon energy ($h\upsilon$) through the Tauc's relation[20].

$$\alpha h\upsilon = A\,(h\upsilon - Eg)^{1/2} \tag{2}$$

The optical band gap energy (E_g) of 3-AP crystal was found to be 4.5 eV from the Tauc's plot which is shown in Figure 4.

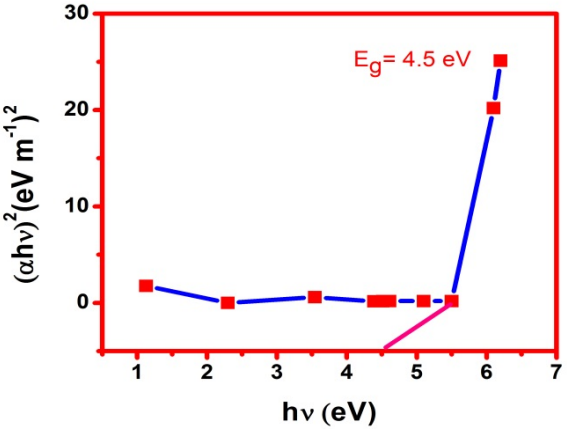

Fig 4. Tauc's plot

The value of the wide band gap indicates its suitability for optoelectronics applications[21]. Theoretically, the optical band gap energy of 3-AP crystal was calculated using the following relations:

$$E = \frac{hc}{\lambda} \tag{3}$$

where λ is the lower cut-off wavelength (250 nm). The band gap of the grown crystal is found to be 4.96 eV.

3.3.2 Determination of Optical Constants

The reflectance (R) gives the ratio of the energy reflected to incident light from the crystal. The reflectance R in terms of absorption coefficient (α) and the thickness of the crystal (t) can be determined using the relation

$$R = 1 \pm \frac{\sqrt{1 - exp(-\alpha t) + exp(\alpha t)}}{1 + exp(-\alpha t)}$$

Equation can be used to calculate the refractive index n using reflectance data.[22]

$$n = \frac{-(R+1) \pm \sqrt{-3R^2 + 10R - 3}}{2(R-1)}$$

The calculated refractive index (n) value using the above equations for the grown 3-AP is 2.72. Figure 5 shows the reflectance as a function of wavelength graphically. The reflectance (R) of the crystal was calculated using the following relation

$$R = \frac{(n-1)^2}{(n+1)^2}$$

The calculated value of reflectance (R) is 0.2134. Reflectance as a function of wavelength is graphically illustrated in Figure 5.

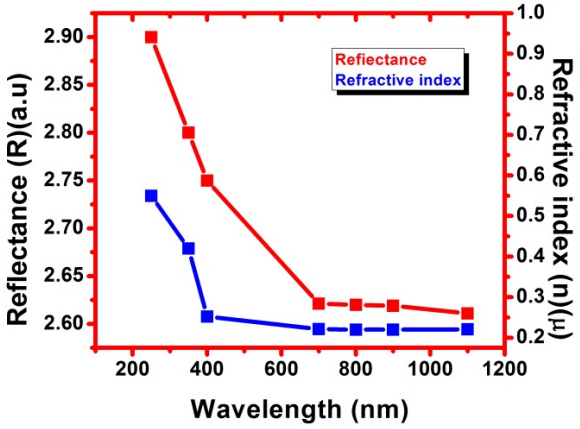

Fig 5. Wavelength vs reflectance and wavelength vs refractive index

3.3.3 Optical Conductivity

Optical conductivity is one of the powerful tools for studying the electronic states in materials. Based on the relation, the optical conductivity (σ_{op}) has been calculated.

$$\sigma_{op} = \alpha nc/4\pi \tag{4}$$

The variation of optical conductivity with wavelength is shown in Figure 6. As the wavelength increases optical conductivity decreases.

3.3.4 Electrical Conductivity

The electrical conductivity of a material is related to the optical conductivity of the crystal using the following equation:

$$\sigma_e = 2\lambda\sigma_{op}/\alpha \tag{5}$$

The variation of electrical conductivity with wavelength is shown in Figure 6. As the wavelength increases electrical conductivity increases.

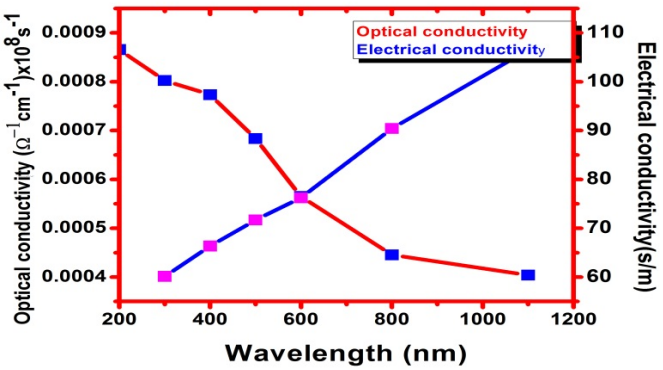

Fig 6. Plot of λ versus

3.3.5 Electric Susceptibility

The electric susceptibility (χ_c) values are estimated using the calculated extinction coefficient and refractive index values of 3-AP crystal by the below relation:

$$\varepsilon_r = \varepsilon_0 + 4\pi\chi_c = n^2 - k^2 \tag{6}$$

$$\chi c = (n^2 - k^2 - \varepsilon_0)/4\pi \tag{7}$$

Where ε_0 is the permittivity in free space. The complex dielectric constant is given by ε_c. The real and imaginary part of the dielectric constant from the extinction coefficient is given as

$$\varepsilon_c = \varepsilon_r + i\varepsilon_i \tag{8}$$

$$\varepsilon_r = n^2 - k^2 \tag{9}$$

$$\varepsilon_i = 2nk \tag{10}$$

Where ε_r and ε_i are real and imaginary parts of the dielectric constant. The electric susceptibility is calculated as χ_c = 5.8214. The real ε_r and imaginary ε_i values of the dielectric constant are 7.4158 and 3.0991x10^{-6}

3.4 Fluorescence Analysis

Compounds that are aromatic or have several conjugated double bonds with a high degree of resonance stability exhibit fluorescence. Fluorescence analysis is the most important nondestructive method for assessing the energy state transitions, surface interfaces, and flaws in materials[23]. It therefore finds huge application in biomedical and photonics. The fluorescence spectrum of the grown 3-AP crystal was recorded in the range of 300 nm to 900 nm using the Perkin Elmer model LS-45

fluorescence spectrometer. Figure 7 shows the 3-AP emission spectrum. There are four categories of fluorescence peaks in the spectra. The first emission peak is observed at 361 nm which is due to visible violet. Violet light is used in applications including optical disc drives, and violet lasers are used in blue-ray disc players, optical disc drives, and optical communication systems. Violet and ultraviolet light are being used for high-speed data transmission. The second peak at the wavelength of 468 nm is due to the emission of blue. The sharp peak at 648 nm shows the emission of red and the peak at 778 nm is due to the emission of red. Red fluorescence is used in a variety of applications including analytical fluorimetry and biomedical research.

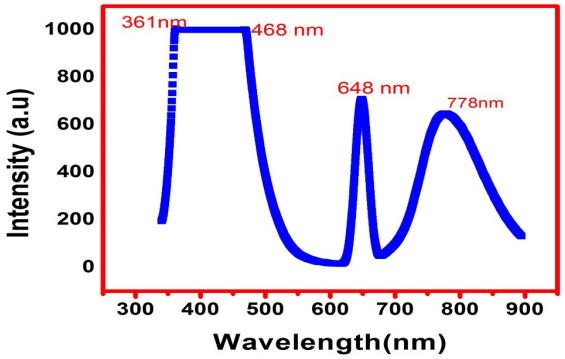

Fig 7. Fluorescence emission spectrum of 3-AP

3.5 TGA/DTA/DSC

Thermal behavior provides information on the crystal's stability and melting point. The TGA curve gives the quantitative measurement of mass change associated with the transition. The thermal stability of 3-AP crystal was screened by a Perkin-Elmer Thermo Gravimetric Analyzer (TGA) with Differential Thermal Analysis (DTA) in the air atmosphere with a heating rate of 2 °C / min with the temperature range of 50 °C to 800 °C as shown in Figure 8. The absence of water in the molecular structure during crystallization is confirmed by the absence of weight loss at 100 °C. The 3-AP crystal remains stable up to 220 °C and then the crystal begins to decompose up to 260 °C due to the loss of NH_2 group of the 3-aminopyridine and the total weight loss of the compound is 65 %. Further decomposition begins at the temperature of 255 °C and considerable weight loss is observed at the temperature of 800 °C, is due to the volatilization and decomposition of the material. The good thermal stability of 3-AP crystal indicates that it can be used as a candidate for device fabrication in optoelectronics. The recorded TGA and DTA spectrum of a 3-AP single crystal is shown in Figure 7.

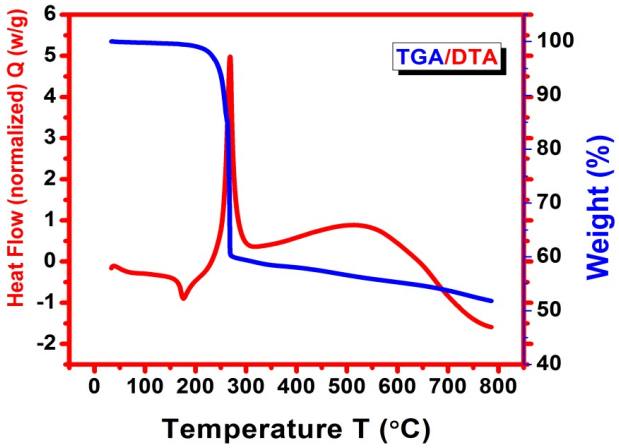

Fig 8. TGA/DTA curve of 3-AP

It is observed from the DTA spectrum, that endothermic and exothermic peaks are noticed at 185 °C and 260 °C respectively. This is followed by an exothermic peak at 260 °C which coincides with decomposition observed in the TGA curve. The sharpness of the peak shows a good degree of crystallinity in the sample. The results of TGA and DTA show that the material can be used for optoelectronic applications up to 185 °C.

3.6 Microhardness Analysis

Microhardness study was carried out in the 3-AP crystal for various loads from 10 to 100 g with a constant time of indentation (10s) using a Shimadzu MHV-G21 micro hardness tester fitted with diamond pyramidal indenter. The diagonal length was measured for each instance, and the average was determined. The Vickers hardness parameter (H_v) is calculated using the formula [24]

$$H_v = \frac{1.8544\, x\, P}{d^2}\, kg/mm^2 \tag{11}$$

where P is the applied load and d is the average diagonal length of indentation. For an applied load above 100 g, the crystal begins to crack. A graph was plotted between H_v versus load P as shown in Figure 9. This demonstrates that when the stress increases, the hardness value decreases, which indicates that 3-AP exhibits a normal indentation size effect (ISE). The load and indentation diagonal length are related by Meyer's law, which is used to calculate Meyer's index number [24]

$$P = A = Kd^n \tag{12}$$

where A is an arbitrary constant.

$$\log P = \log K + n \log d \tag{13}$$

Here, K is the material constant and n is Meyer's index (or) work hardening coefficient, which characterizes the material category. Figure 9 shows the plot of log P versus log d fitting data using the least-squares fit method and the value of n was found to be 2. Since the work hardening coefficient of the developed crystal in this study is more than 1.6, the grown crystal 3-AP belongs to the soft material and will thus readily permit light to pass through [25].

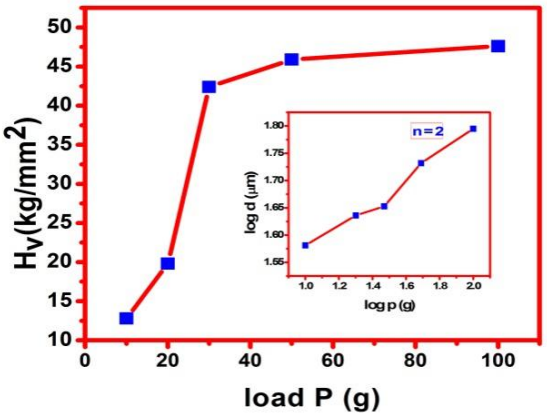

Fig 9. Load P versus hardness number H_v and log d versus log P

3.7 Dielectric Analysis

The dielectric studies on 3-AP crystal have been carried out using Jognic's Model 2816B LCRZ Meter. The presence of all polarizations including space charge, orientation, and electric and ionic polarizations can be responsible for the high dielectric constant value at low frequencies [26]. The material absorbs electrical energy which then dissipates as heat. This dissipation of energy is called dielectric loss [27] Equation $\varepsilon' = \varepsilon \tan \delta$ has been used to calculate the crystal's dielectric loss; ε is the dielectric constant and tan δ is the dispersion power factor. It may be that in a certain frequency range $\omega_4 < \omega < \omega_5$, the value

of $\varepsilon'(\omega)$ becomes negative; this corresponds to the high dielectric strength of the oscillator and its low damping. Frequency dependence of losses (ε'') in the range of dispersion is characterized by a maximum at frequency $\omega = \omega_6$. The plot of frequency versus dielectric constant and dielectric loss is shown in Figure 10. With the low dielectric loss and dielectric constant at high frequencies, this material can be used in optical applications.

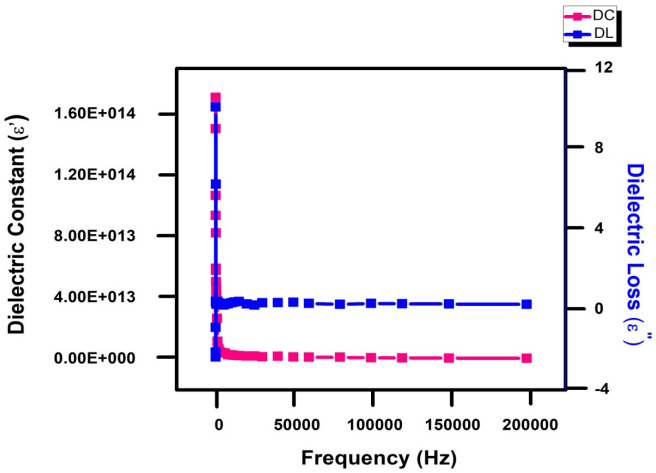

Fig 10. Variation of dielectric constant and dielectric loss with frequency

4 Conclusion

This study presents evidence for the 3-aminopyridine crystal as a suitable candidate for optoelectronic device fabrication. A brown color crystal of 3-aminopyridine (3-AP) was grown by the slow evaporation method. The single-crystal XRD diffraction studies show that the grown crystal belongs to a monoclinic crystal system. The functional group NH_2 present in the 3-AP single crystal was identified by FTIR spectral study. The UV-visible NIR transmittance spectrum shows the lower cut-off wavelength at 250 nm. The lower cut-off wavelength, very good transmittance in the UV, the entire visible region, and the near-infrared region indicate the suitability of the 3-AP crystal for optoelectronic applications. The band gap energy is calculated as 4.5 eV from Tauc's plot. The optical characteristics of the crystal such as reflectance, refractive index, susceptibility, optical conductivity, and electrical conductivity were computed from the UV-Vis NIR spectral studies. Fluorescence spectral analysis shows the emission of violet and red emission thus confirming the suitability of the 3-AP crystal for optoelectronic device fabrication. The thermal stability of the 3-AP is high as 220 °C which is an important requisite for optoelectronic device fabrication. Vickers hardness test shows the crystal belongs to soft type material. The dielectric constant of the 3-AP crystal is high at low frequencies due to the space charge polarization. The dielectric loss is minimal at high log frequency indicating that the crystal is suitable for optoelectronic device fabrication. From the above studies, it is confirmed that the 3-AP crystal is a potential candidate for optical and photonic device fabrication.

References

1) Aarthy J, Suriya M, Murugesan KS, Boaz M, B. Studies on the Growth, Optical, Thermal and Physical Properties of an Efficient Second Order Nonlinear Optical Organic Crystal, 2-Amino-5-ChloropyridiniumTrifluoroacetate for Optoelectronic and Photonic Device Applications. *Indian Journal of Pure & Applied Physics*. 2022;60:763–772. Available from: https://doi.org/10.56042/ijpap.v60i9.59681.
2) Kavitha E, Karnan C, Manivannan S, Madhavan J. Synthesis, crystal structure, vibrational, optical, thermal and photoluminescence properties of di bromide bis {2-[(2-chlorophenyl) methylidene] hydrazine-1-carbothioamide}-cadmium [CdL2Br2. *Chemical Data Collections*. 2021;31:100594–100594. Available from: https://doi.org/10.1016/j.cdc.2020.100594.
3) Aijaz A, Shaista D, H, Ishtiyaq L, A, Aadil A, et al. Engineering the solid-state luminescence of organic crystals and co crystals. *Advanced Materials*. 2024;5. Available from: https://doi.org/10.1039/d3ma00853c.
4) Wu M, Zhuang Y, Liu J, Chen W, Li X, Xie R. Ratiometric fluorescence detection of 2, 6-pyridine di carboxylic acid with a dual-emitting lanthanide metal-organic framework (MOF). *Optical materials*. 2020;106:11006–11006. Available from: http://dx.doi.org/10.1016/j.optmat.2020.110006.
5) Surya S, Sindhusha S, Ramasamy P, Karuppasamy P, Gunasekaran B. Investigation on growth, crystal structure third order optical nonlinearity properties and DFT computational studies of novel proton transfer 3-aminopyridine P-Nitro benzoate P-Nitro benzoic acid (3-APPNB) single crystal for third order Nonlinear optical applications. *Journal of photochemistry and photobiology A: chemistry*. 2023;111:114908–114908. Available from: https://doi.org/10.1016/j.jphotochem.2023.114908.

6) Kaliammal R, Parvathy G, Maheswaran G, Sankaranarayanan K, Arivanandhan M, Sudhahar S. Crystal growth, structural, optical, thermal, and mechanical properties of new bis (2-amino-6-methyl pyridinium barbiturate) tetrahydrate organic single crystal for nonlinear optical applications. *Chinese journal of physics*. 2020;68:436–460. Available from: https://doi.org/10.1016/j.cjph.2020.09.027.
7) De S, Kumar A, K S, Shah SK, Kazi S, Sarkar N, et al. Pyridine: the scaffolds with significant clinical diversity. *RSC Advances*. 2022;12. Available from: https://doi.org/10.1039/d2ra01571d.
8) Nimmy L, John S, Aswathy PAJG, Subramani S, V. Growth, quantum mechanical computations, NLO and spectroscopic, studies of 2-amino 5-chloro pyridine single crystal in comparison with certain amino pyridine derivatives. *Journal of Molecular structure*. 2023;1272:134120. Available from: https://doi.org/10.1016/j.molstruc.2022.134120.
9) Ravi S, Raghi KRRS, Kumar TKM, Naseema K. Transition Experimental and Theoretical Studies on Various Linear and Non-linear Optical Properties of 3-Aminopyridinium 3, 5-Dinitrobenzoate for Photonic Applications. *Metal Chemistry*. 2021;46:191–200. Available from: https://doi.org/10.1007/s11243-020-00436-2.
10) Panchapakesan S, Subramani K, Srinivasan B. Growth, characterization and quantum chemical studies of an organic single crystal: 3-Aminopyridine 4-Nitrophenol for opto-electronic applications. *Journal Material science and materials in electronics*. 2017;28:5754–5775. Available from: https://link.springer.com/article/10.1007/s10854-016-6247-x.
11) Mohanbabu B, Bharathikannan R, Siva G. Investigations on structural, optical, electrical, mechanical and third-order nonlinear behaviour of 3-aminopyridinium, 4-dinitrophenolate single crystal. *Journal of Applied Physics A*. 2017;123:1–10. Available from: https://doi.org/10.1007/s00339-017-1262-1.
12) Surya S, Sindhusha S, Gunasekaran B. Synthesis, structural, optical, thermal, electrical, nonlinear optical and theoretical investigations on 3-aminopyridine picrate (3-APP) single crystal. *Journal of molecular structure*. 2023;1272:134259–134259. Available from: https://doi.org/10.1016/j.molstruc.2022.134259.
13) Bindulekha SR, Bai JS, Sindhusha S, S. Experimental and theoretical interpretations of structural, optical, mechanical and thermal properties of 2-aminopyridinium phthalate single crystals. *Chemical Physics Impact*. 2024;8:10058–10058. Available from: https://doi.org/10.1016/j.chphi.2024.100548.
14) Raju E, Jayaprakash P, Purushothaman P, Vinitha G, Devi NS, Kumaresan S. Linear and nonlinear optical properties of 2-Aminopyridinium fumarate fumaric acid single crystal for optoelectronic device applications. *Chemical Physics Letters*;780:138941–138941. Available from: https://doi.org/10.1016/j.cplett.2021.138941.
15) Irfan A, Chaudhry AR, Al-Sehemi AG, Assiri MA, Hussain A. Charge carrier and optoelectronic properties of phenylimidazo [1, 5-a] pyridine-containing small molecules at molecular and solid-state bulk scales computational. *Materials science*. 2019;179:109179–109179. Available from: https://doi.org/10.1016/j.commatsci.2019.109179.
16) Chao M, Schemp E, Rosenstein R, ;. 3-Aminopyridine. *Acta crystallography B*. 1975;31:2924–2926. Available from: https://doi.org/10.1107/S0567740875009284.
17) Chou S, Lu JYPHC, Cheng B. Cheng Electronic and Vibrational Absorption Spectra of NH2 in Solid Ne. *ACS Omega*. 2019;4:2268–2274. Available from: https://doi.org/10.1021/acsomega.8b03344.
18) Ramachandran K, Raja A, Kumar VM, Pandian MS, Ramasamy P. Growth and characterization of 4-methyl-3-nitrobenzoic acid (4M3N) single crystal by using vertical transparent Bridgman-Stock Barger method for NLO applications. *Physica b: Condensed Matter*. 2019;562:82–93. Available from: https://doi.org/10.1016/j.physb.2019.03.014.
19) Senthil A, Bharanidharan T, Vennila M, Elangovan K, Muthu S. Crystal growth, Hirshfeld analysis, optical, thermal, mechanical, and third-order non-linear optical properties of Cyclohexyl ammonium picrate (CHAP) single crystal. *Heliyon*. 2024. Available from: https://doi.org/10.1016/j.heliyon.2024.e28002.
20) Bychto L, Maliński M. Determination of the Optical Absorption Coefficient Spectra of Thin Semiconductor Layers from Their Photoacoustic Spectra. *International Journal of Thermophysics*. 2018;39(9):103–103. Available from: https://dx.doi.org/10.1007/s10765-018-2424-x.
21) Yang J, Liu K, Chen X, Shen D. Recent advances in optoelectronic and microelectronic devices based on ultrawide-bandgap semiconductors. *Progress in Quantum Electronics*. 2022;83:100397–100397. Available from: https://dx.doi.org/10.1016/j.pquantelec.2022.100397.
22) Bincy P, Srinivasan T, S J. Ram kumar V. Structure, growth and characterization of a new naphthalene family crystal for fluorescence and third order nonlinear optical applications. *Solid State Physics*. 2019;89:85–92. Available from: https://doi.org/10.1016/j.solidstatesciences.2018.12.024.
23) Shalini M, Sundararajan RS, Manikandan E, Meena M, Ebinezer BS, Girisun TCS, et al. Growth and characterization of L-Methionine Barium Bromide (LMBB) semi-organic crystal for optical limiting applications. *Optik-International Journal for Light and Electron Optics*. 2023;278:170705–170705. Available from: https://doi.org/10.1016/j.ijleo.2023.170705.
24) Mendoza-Galván A, Méndez-Lara JG, Mauricio-Sánchez RA, Jarrendahl K, Arwin H. Effective absorption coefficient and effective thickness in attenuated total reflection spectroscopy. . *optics letters*. 2021;46:872–875. Available from: https://doi.org/10.1364/OL.418277.
25) Farhat S, Rekaby M, Awad R. Vickers micro hardness and indentation creep studies for erbium doped ZnO nanoparticles. *SN Applied Sciences*. 2019;1:546–546. Available from: https://doi.org/10.1007/s42452-019-0559-4.
26) Raj KK, Kumar NS, Kumar PP. Growth, spectral, mechanical, electrical and optical characterization of guanidinium hydrogen succinate single crystal. *Bulletin of Material Science*. 2020;43:41–41. Available from: https://doi.org/10.1007/s12034-019-201.
27) Gunjan V, Jigar S, Shery J. DoE implementation for Telmisartan and hydrochlorothiazide drug-drug co crystal synthesis to enhance physicochemical and pharmacokinetic properties. *Journal of Applied Pharmaceutical Science*. 2023;13:67–076. Available from: https://doi.org/10.1007/s10765-018-2424-x.